Band-gap engineering of $La_{1-x}Nd_xAlO_3$ ($x = 0, 0.25, 0.50, 0.75, 1$) perovskite using density functional theory: A modified Becke Johnson potential study

Sandeep[1,†], D P Rai[2], A Shankar[3], M P Ghimire[4], Anup Pradhan Sakhya[5], T P Sinha[5], R Khenata[6], S Bin Omran[7] and R K Thapa[1]

[1] *Department of Physics, Mizoram University Aizawl-796004, India*
[2] *Department of Physics, Pachhunga University College, Aizawl-796001, India*
[3] *Department of Physics, University of North Bengal, Darjeeling-734013, India*
[4] *Condensed Matter Physics Research Center, Butwal, Rupandehi, Nepal*
[5] *Department of Physics, Bose Institute, 93/1 Acharya Prafulla Chandra Road, Kolkata 700009, India*
[6] *Laboratoire de Physique Quantique et de Modélisation Mathématique (LPQ3M), Departement de Technologie, Université de Mascara, 29000 Mascara, Algerie, Algeria*
[7] *Department of Physics and Astronomy, College of Science, King Saud University, P. O. Box 2455, Riyadh 11451, Saudi Arabia*

(Received 24 May 2015; revised manuscript received 9 February 2016; published online 20 April 2016)

The structural, electronic, and magnetic properties of the Nd-doped Rare earth aluminate, $La_{1-x}Nd_xAlO_3$ ($x = 0\%$ to 100%) alloys are studied using the full potential linearized augmented plane wave (FP-LAPW) method within the density functional theory. The effects of the Nd substitution in $LaAlO_3$ are studied using the supercell calculations. The computed electronic structure with the modified Becke–Johnson (mBJ) potential based approximation indicates that the $La_{1-x}Nd_xAlO_3$ alloys may possess half-metallic (HM) behaviors when doped with Nd of a finite density of states at the Fermi level (E_F). The direct and indirect band gaps are studied each as a function of x which is the concentration of Nd-doped $LaAlO_3$. The calculated magnetic moments in the $La_{1-x}Nd_xAlO_3$ alloys are found to arise mainly from the Nd-4f state. A probable half-metallic nature is suggested for each of these systems with supportive integral magnetic moments and highly spin-polarized electronic structures in these doped systems at E_F. The observed decrease of the band gap with the increase in the concentration of Nd doping in $LaAlO_3$ is a suitable technique for harnessing useful spintronic and magnetic devices.

Keywords: density functional theory, rare earth aluminates, perovskites, electronic structures

PACS: 71.15.–m, 71.15.Mb, 71.20.Eh, 74.62.Dh **DOI:** 10.1088/1674-1056/25/6/067100

1. Introduction

Compounds with perovskites structure, ABX_3 have been the subject of tremendous study due to their diverse applications.[1,2] These applications range from ferro- and piezoelectricity,[3] high electronic and ionic conductivity, diverse magnetism, colossal magnetoresistive effects,[4] to paraelectricity and superconductivity. Single crystalline substrates of $RAlO_3$ alloys such as $LaAlO_3$ and $YAlO_3$ are commonly used for the epitaxy of thin films such as high-temperature superconductor (HTSC), magnetoresistive materials, and GaN films.[5] The effects of doping on the structural, electronic, transport, magnetic, and specific heat properties in 4d perovskites were studied by Zhang *et al.*,[6] where $YAlO_3$ doped with Yb-2p or V-4p was proposed as a material for tunable solid-state laser.[7,8] Dielectric permittivities with 'high-quality factor' are of prime interest among rare earth aluminates as they are appropriate for dielectric resonators and substrates for microwave components.[9–11] Recent developments in electronics,[12] optics,[13] and energy conversion applications[14] using the ABO_3 type of perovskite compounds have aroused the renewed interest in this field. $LaAlO_3$ is used as the superconductive substrate, superconducting microwave devices, and high k gate oxide to replace silicon dioxide (SiO_2) because of its good dielectric characteristics, and thermal properties.[15] At room temperature, $LaAlO_3$ is stable in the rhombohedral structure with $R3c$ space group. By using $LaAlO_3$ as a host material for phosphor where it is doped with transition metals for multiferroic properties, the $LaAlO_3$ turns into an important material to be explored theoretically as well as experimentally.[13] Limited studies have been observed to date on the ferromagnetic and optical properties of the transition metal-doped $LaAlO_3$.[16–18] Hong-Sheng *et al.* studied the modification of the band gap in β-SiC and reported the change from indirect to direct band gap and the decrease of the energy band gap with doping the N-atom for the C atom.[19] Fang *et al.* have satisfactorily explained the manifestation of an addi-

*Project supported by the DST-SERB, Dy (Grant No. SERB/3586/2013-14), the UGCBSR, FRPS (Grant No. F.30-52/2014), the UGC (New Delhi, India) Inspire Fellowship DST (India), and the Deanship of Scientific Research at King Saud University (Grant No. RPG-VPP-088).

†Corresponding author. E-mail: sndp.chettri@gmail.com

tional absorption peak in the experiments through the doping studies of $KMgF_3$.[20] On the other hand, Shu-Lai *et al.* have analyzed the weakening of the magnetic moment and magnetic stabilized energy in defective graphene with the hydrogen chemisorbed single-atom vacancy (H-GSV).[21] The decrease in the conductivity of ZnO was predicted and compared with the experimental results by Hou Qing-Yu *et al.*[22] using the pseudopotential method. Optical properties of TiO doped with two atoms were studied by Wang Qing *et al.*[23] and Shi-Bin *et al.* studied the effect of polarization doping of AlGaN and predicted that it is a more efficient doping technique.[24] Zylberberg and Ye[25] have studied the dielectric properties of bismuth-doped $LaAlO_3$ to correlate the higher dielectric properties using the high polarizability of the Bi^{3+} ion with a lone electron pair. Conversely, the structural and optoelectronic properties were studied by Murtaza and Ahmad[26] to explain the shift from the indirect to direct band gap under pressure for $LaAlO_3$. Namjoo *et al.*[27] have studied the structural, electronic and optical properties of InAs, InSb, and their ternary alloys, $InAs_xSb_{1-x}$ ($x = 0.25, 0.5, 0.75$) within the density functional theory using the modified Becke–Johnson exchange–correlation functional (mBJ-LDA),[28] to report the concentration at which the minimum band gap occurs. In addition, $LaAlO_3$ having the structure, *Pm*-3*m* is the stablest structure at its ground state which is favorable for making layered structures and doped structures for technological application. As $LaAlO_3$ and $NdAlO_3$ are already studied and reported as suitable candidates for optoelectronic devices, we attempt to see the significant changes in its electronic structure and phase transitions as we vary the atoms from La to Nd.

2. Method of calculation

The calculations reported here are carried out using the *ab initio* full-potential linearized augmented plane wave (FP-LAPW) method[29,30] as implemented in the WIEN2k code,[31] which is one of the most efficient methods of calculating and simulating the ground state properties of materials.[32] Owing to the flexible basis sets in the interstitial and near atomic centers, this method is well suited for open structures with low symmetry. The exchange potential was calculated using the modified Becke–Johnson exchange potential[28–38] and the core states were treated relativistically while the valence states were treated with a scalar relativistic approximation. We employ well-converged basis sets, defined by $R_{\min}K_{\max} = 7.0$, where $R_{\min}$ is the smallest sphere radius and $K_{\max}$ is the interstitial plane-wave cutoff. Local orbitals were employed to include the semi-core states and to efficiently linearize the s and p states of the Al and O atoms.[39] A supercell approach[40] was used for doping $LaAlO_3$ with the Nd atoms where it was constructed by substituting one Nd atom in place of the La atom within the unit cell of $LaAlO_3$. We generate 8 La atoms using supercells with the $2 \times 2 \times 2$ configuration and the Nd element is doped at the La site within the unit cell of $LaAlO_3$ as $La_{1-x}Nd_xAlO_3$. The x compositions are varied such as 25% (2/8), 50% (4/8), 75% (6/8), and 100% (8/8), respectively, as shown in Figs. 1(a)–1(e). When doping, the system undergoes structural phase transition[41] from the space group, *Pm*-3*m* to the space group,*P4/mmm*. The Nd atom has 4f electrons which contribute to the electronic and magnetic feature of the doped system.

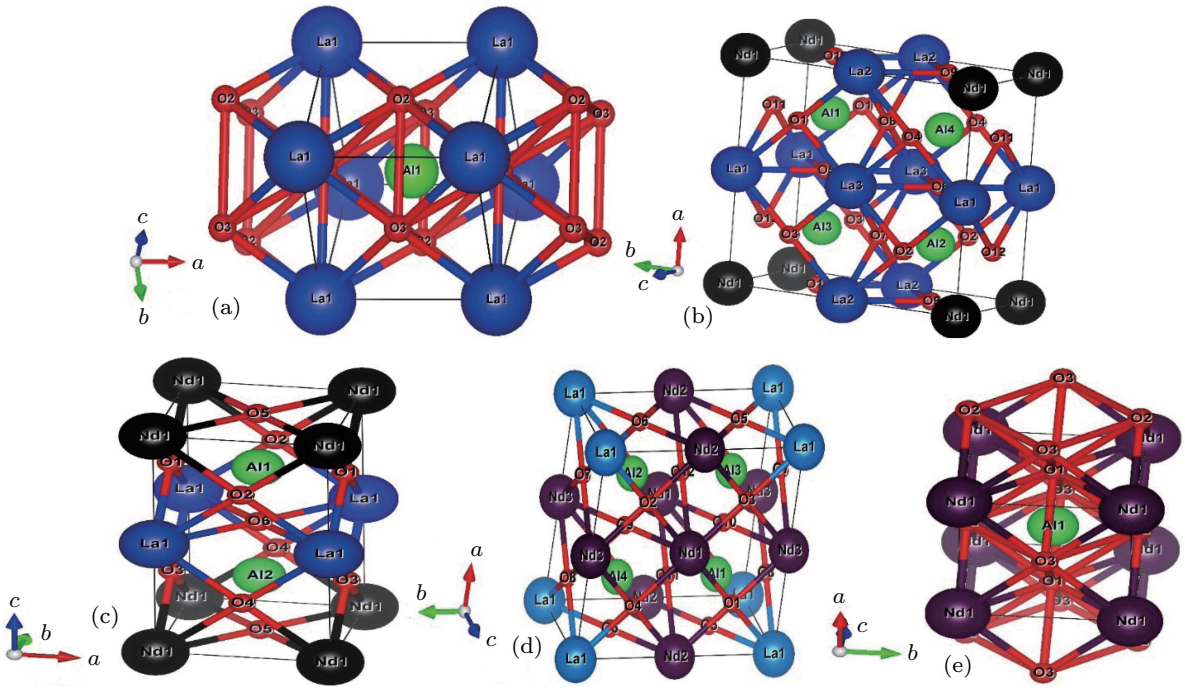

Fig. 1. Fig. 1. Supercells of the $La_{1-x}Nd_xAlO_3$ alloys with (a) $x = 0\%$ or (0/8), (b) $x = 25\%$ or (2/8), (c) $x = 50\%$ or (4/8), (d) $x = 75\%$ or (6/8), and (e) $x = 100\%$ or (8/8).

3. Results and discussion

3.1. Volume, bulk modulus, pressure derivative, and energy

The total energies of the $La_{1-x}Nd_xAlO_3$ alloys are calculated each as a function of the volume using the full potential linearized augmented plane wave method, where the plots of the calculated total energies versus the reduced volume for these alloys are given in the following Figs. 2(a)–2(e).

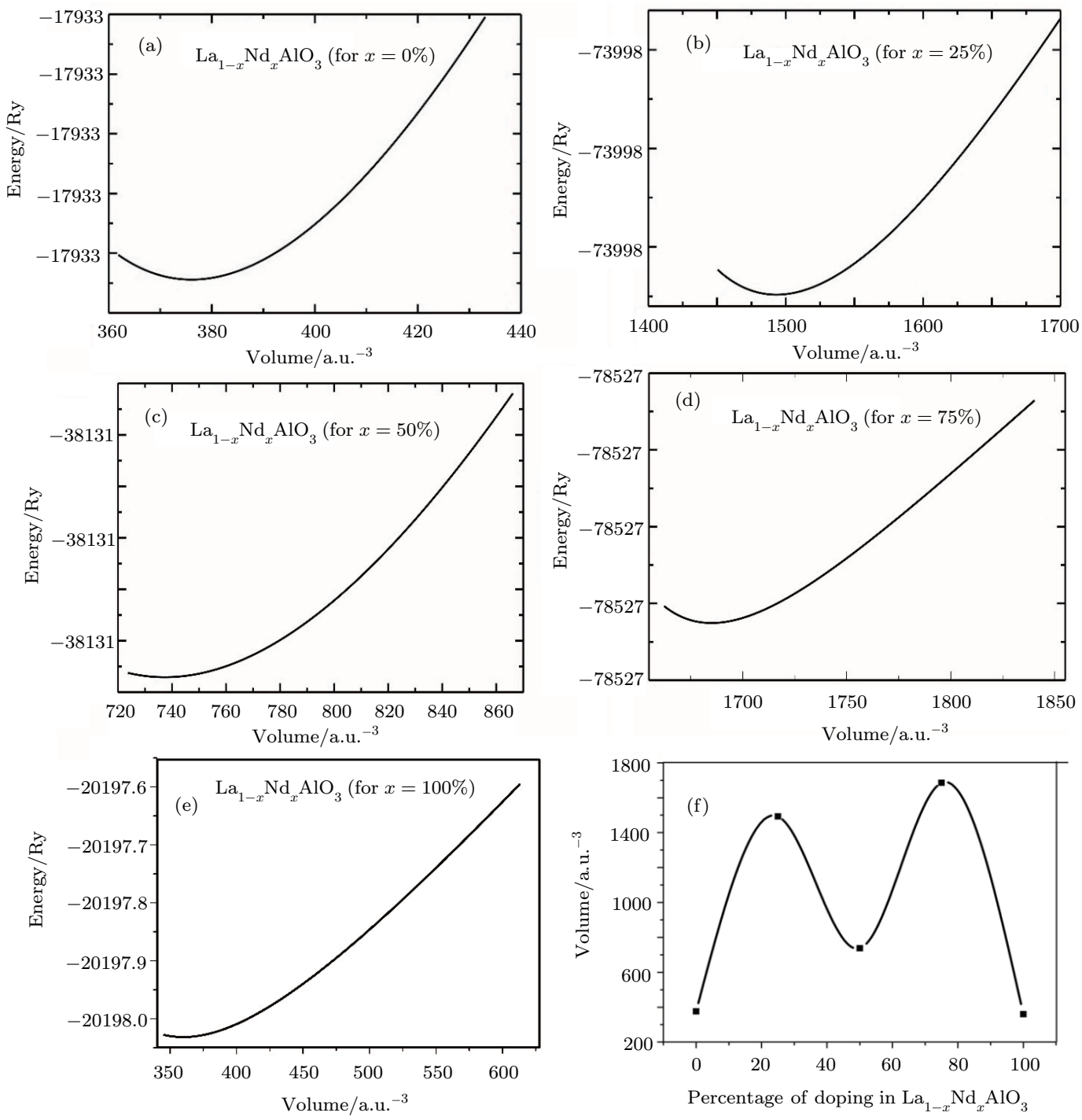

Fig. 2. Fig. 2. Plots of energy versus volume for $La_{1-x}Nd_xAlO_3$ alloys with (a) $x = 0\%$ or (0/8), (b) $x = 25\%$ or (2/8), (c) $x = 50\%$ or (4/8), (d) $x = 75\%$ or (6/8), (e) $x = 100\%$ or (8/8), and (f) plot of the percentage of Nd doping vs volume for the $La_{1-x}Nd_xAlO_3$ alloys.

The calculated total energies are fitted to the Murnaghan's equation of state[42] to determine the ground state properties, such as the equilibrium volume (V), the bulk modulus (B), its pressure derivative (BP), and energy (E). The calculated equilibrium parameters such as V, B, BP, and E, are given in the following Table 1, which also contains the available experimental and theoretical results for comparison with other literatures.[43–45]

Table 1. Lattice parameters of the $La_{1-x}Nd_xAlO_3$ alloys, volume, bulk modulus, pressure derivatives, and energy.

$La_{1-x}Nd_xAlO_3$	Volume/a.u.^{3}	B/GPa	BP	Energy/Ry
$x = 0\%$	376.0695	206.4012	6.1550	−17933.27
	375.7952[43]	196.03[45]	4.1506[43]	−17933.27[45]
		185.63[45]		
	368.2565[44]	195.76[45]		
		190[44]		
$x = 25\%$	1493.2134	259.4682	14.5616	−73997.87
$x = 50\%$	737.3292	189.1335	4.2217	−38131.31
$x = 75\%$	1685.0617	1673.0579	46.7058	−78527.22
$x = 100\%$	359.8465	180.7324	4.8296	−20198.03

We find that the volume of the system increases, in general from 1493.2134 a.u.^{3} at 25% to 1685.0617 (a.u.)^3 at 75% doping of Nd in $LaAlO_3$. Also at doping levels of 0%, 50%, and 100%, the volumes are found to be 376.0695 a.u.^{3}, 737.3292 a.u.^{3}, and 359.8465 a.u.^{3}, respectively. A similar trend in the bulk moduli and the respective derivatives of the bulk moduli are also observed as shown in Table 1. Similarly, the bulk moduli of the $La_{1-x}Nd_xAlO_3$ alloys are found to have a relative increase of 25%, a relative decrease of 8.37%, a relative increase of 710%, and a relative decrease of 14.20%, respectively, from $x = 0\%$ to $x = 25\%$, 50%, 75%, and 100% of Nd doping. These changes can be attributed to the size difference or the mismatch of the size of the crystallites with doping and similar trends in the pressure derivatives and energies are also observed in these systems.

3.2. Density of states

For $La_{1-x}Nd_xAlO_3$ (at $x = 0\%$), the densities of states (DOSs) respectively, in the spin-up and spin-down configurations show similar features where the top of the valence band extending from −3.0 eV to the Fermi level (E_F) is dominated mostly by the O-2p state hybridized with the Al-2p state. Conversely, the conduction band which starts from 4.5 eV is mainly composed of the 4f orbital. In all the dopant concentrations, the orbital character of the valence band is primarily derived from the O-2p state orbital.

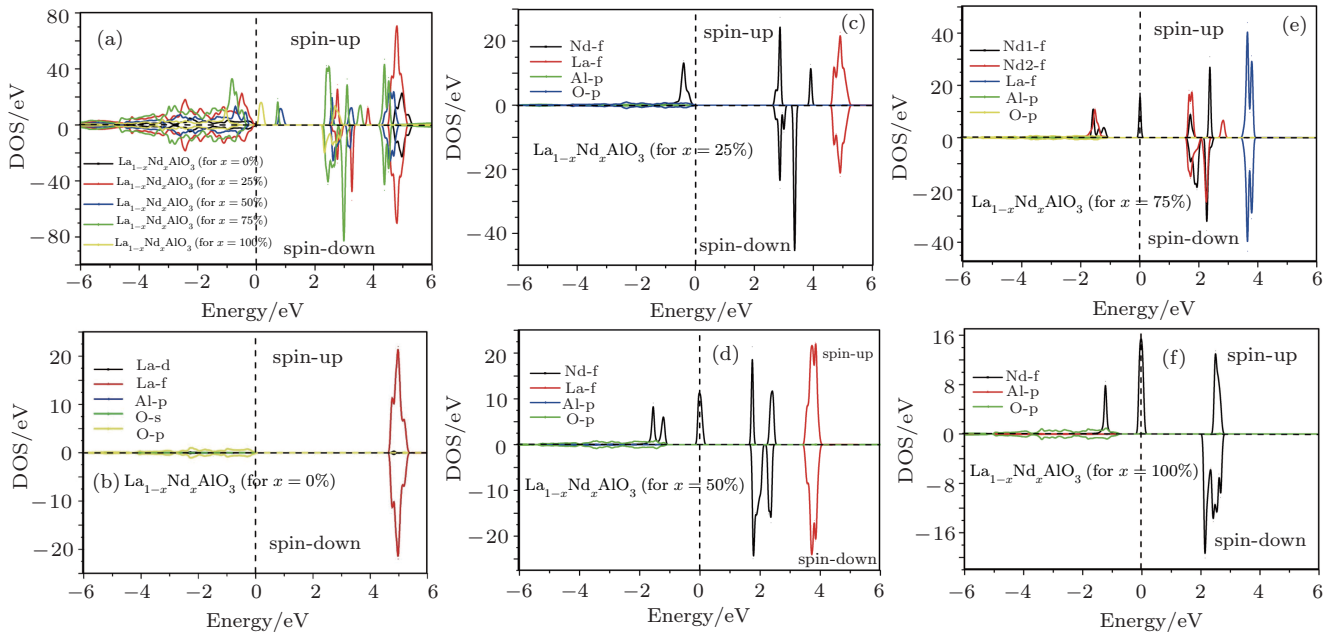

Fig. 3. (color online) (a) Total DOS plots of the $La_{1-x}Nd_xAlO_3$ alloys ($0\% < x < 100\%$); the partial DOS plots of the La-d, La-f, Al-p, O-s, and O-p states of the $La_{1-x}Nd_xAlO_3$ alloys at $x = 0\%$ (b), 25% (c), 50% (d), 75% (e), and 100% (f).

For $La_{1-x}Nd_xAlO_3$ (at $x = 25\%$), in both the spin-up and spin-down channels the lower parts of the valence band remain unchanged with contributions from the O-2p state hybridized with the Al-2p states. The Nd-4f state contributions are observed from −0.5 eV to E_F in the spin-up configuration with a sharp peak at −0.4 eV as shown in Fig. 3(b). In the spin-up channel, the contribution due to the Nd-4f state is observed between 1.75 eV and 4.0 eV with peaks at 2.9 eV in both spin channels and at 3.4 eV in the spin-down channel, and at 4 eV in the spin-up channel, respectively. In both spin channels, the La-4f states contribute between the energies of 4.6 eV to 5.3 eV. For $La_{1-x}Nd_xAlO_3$ (at $x = 50\%$), it is observed that the core and lower valence bands from −5.4 eV to −1.1 eV consist of mainly the Nd-4f states. Sharp peaks due to the Nd-4f states are observed at −1.6 eV and −1.2 eV in the spin-up configurations, respectively. At E_F the sharp peak due to

the Nd-4f state electrons is observed in the spin-up channel. Further peaks are also observed at 2.3 eV in the spin-down configuration, and at 2.4 eV in the spin-up configuration due to the Nd-4f state orbitals, respectively. Conversely, the La-4f state contributions are observed within an energy range from 3.5 eV to 4 eV with sharp peaks at 3.8 eV in both the spin up and spin down channels.

3.3. Band structure, energy band gap, and magnetic moment

Table 2 shows the variations of the direct and indirect band gaps of the $La_{1-x}Nd_xAlO_3$ alloys with concentration. The band gap is found to decrease with the increase of concentration. This is an indication of the fact that the band-gap of $La_{1-x}Nd_xAlO_3$ is tunable using the Nd ion in order to turn $LaAlO_3$ into a promising candidate for optoelectronic applications. The plots of the concentration of doping with respect to band gap as displayed in Fig. 3(b) show a sharp decrease in the magnitude of the band gap for $x = 0\%$, $x = 25\%$, $x = 50\%$, and $x = 75\%$. As the concentration increases, the Nd-4f ions are found to contribute to the insulating[46] band gap of the undoped $LaAlO_3$ as suggested by the density of states plots for the $La_{1-x}Nd_xAlO_3$ alloys as shown in Figs. 3(a)–3(e).

Table 2. Fundamental direct and indirect band gaps of the $La_{1-x}Nd_xAlO_3$ alloys as compared with the previous results.

	Indirect band gap			Direct band gap			Previous results	
$La_{1-x}Nd_xAlO_3$	E_{max}/eV	E_{min}/eV	ΔE_g/eV	E_{max}/eV	E_{min}/eV	ΔE_g/eV	Expt.	Theor.
$x = 0\%$	0.00M	4.65X	4.65	0.00M	4.65M	4.65	5.6[47]	3.19[48]
$x = 25\%$	0.00Γ	2.7R	2.7	0.00Γ	2.85Γ	2.85		
$x = 50\%$	0.10Γ	1.7X	0.60	0.10Γ	1.7Γ	0.60		
$x = 75\%$	0.00Γ	1.6X	1.60	0.00Γ	1.6Γ	1.60		
$x = 100\%$	0.1Γ	2.10X	2.00	0.1Γ	2.40Γ	2.30		

For $La_{1-x}Nd_xAlO_3$ (at $x = 75\%$), the core and lower valence bands are found to be contributed by the Al-2p and O-2p state electrons with an energy of up to -1.0 eV. Both the Nd atoms (Nd-1 and Nd-2) are observed as contributors to the DOS in the valence region of the spin-up channel with peaks at -1.5 eV and E_F (for Nd-2) respectively. In the spin-up configuration, contributions from the Nd-4f states are observed from 1.6 eV to 3.0 eV. The peaks at 1.7 eV in the spin-up channel and spin-down channel are due to both the Nd-4f states, where the peak at 1.9 eV in the spin-down channel is due to Nd-1. Conversely, the peaks at 2.3 eV are due to both Nd atoms in the spin-down channel and the peaks observed at 2.4 eV are due to the Nd1 atom in the spin-up channel. Strong hybridizations between both of these Nd-4f states are observed in both the valence region and the conduction region whereas the La-4f states are found to contribute from 3.4 eV to 3.9 eV in both spin-down channels. The DOS plots show that $La_{1-x}Nd_xAlO_3$ (at $x = 75\%$) participates in maximum hybridization. At E_F, the contributions of the Nd-4f states are observed in the spin-up configuration which indicates that this doping configuration is one of the important resulting systems compared with the remaining configurations. The splitting of the Nd-4f states could be attributed to the magnetic nature of the systems as suggested by the magnetic moments shown in Table 3.

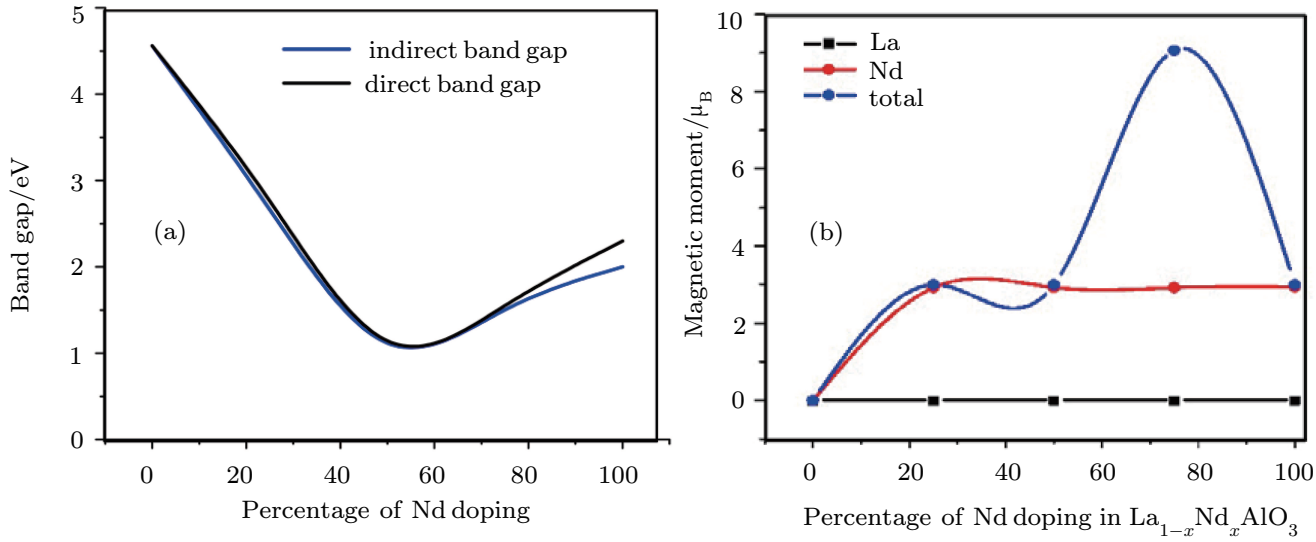

Fig. 4. (a) Plots of direct and indirect band gap versus percentage of Nd doping in $LaAlO_3$ and (b) plots of magnetic moment versus percentage of Nd doping.

It is clearly seen from the figure that $La_{1-x}Nd_xAlO_3$ ($0\% < x < 100\%$) is a direct band gap material.[47] The substitution of the Nd atom does not affect the nature (direct band gap) of the compound but minimizes the gap as shown in Fig. 4(a). It is observed that for $x = 50\%$, 75%, and 100% in $La_{1-x}Nd_xAlO_3$, the spin-down configuration is insulating whereas the mBJ-based electronic structure results clearly predict finite DOS at E_F, for the spin-up configuration. Hence, these doped compounds are predicted to be half-metallic in nature.

In general the major contribution to the DOS of the $La_{1-x}Nd_xAlO_3$ ($0\% < x < 100\%$) alloys is due to the presence of the rare earth ion (Nd-4f) particularly near E_F which has made this system an interesting candidate for doping studies. The direct band gap varies from 4.65 eV to 2.30 eV as shown in Table 2 and the indirect band gap varies from 4.65 eV to 2.00 eV with the doped Nd percentage in $La_{1-x}Nd_xAlO_3$ increasing from 0% to 100% as shown in Fig. 5.

Table 3. Calculated spin magnetizations in units of μ_B of the bulk $La_{1-x}Nd_xAlO_3$ alloys and the supercells, on the basis of transition metal atom La and Nd.

Composition	La1, La2/μ_B	Nd-1, Nd-2/μ_B	Total/μ_B
$x = 0\%$	0.00, –	0.00, –	0.00
$x = 25\%$	0.00, 0.00	2.92, –	3.00
$x = 50\%$	0.00, –	2.93, –	3.00
$x = 75\%$	0.00, –	2.92, 2.92	9.07
$x = 100\%$	–, –	2.94, –	3.00

The variations of the magnetic moment with concentrations are presented in Table 3 and Fig. 4(b). The non-magnetic $LaAlO_3$ at $x = 0\%$ is found to exhibit magnetic ground state when doping with the Nd atoms. The sharp increases in the magnetic moment at $x = 25\%$, 50%, and 75% and the magnetic nature of Nd can be attributed to the manifestation of the density of states at E_F in the spin-up channel.

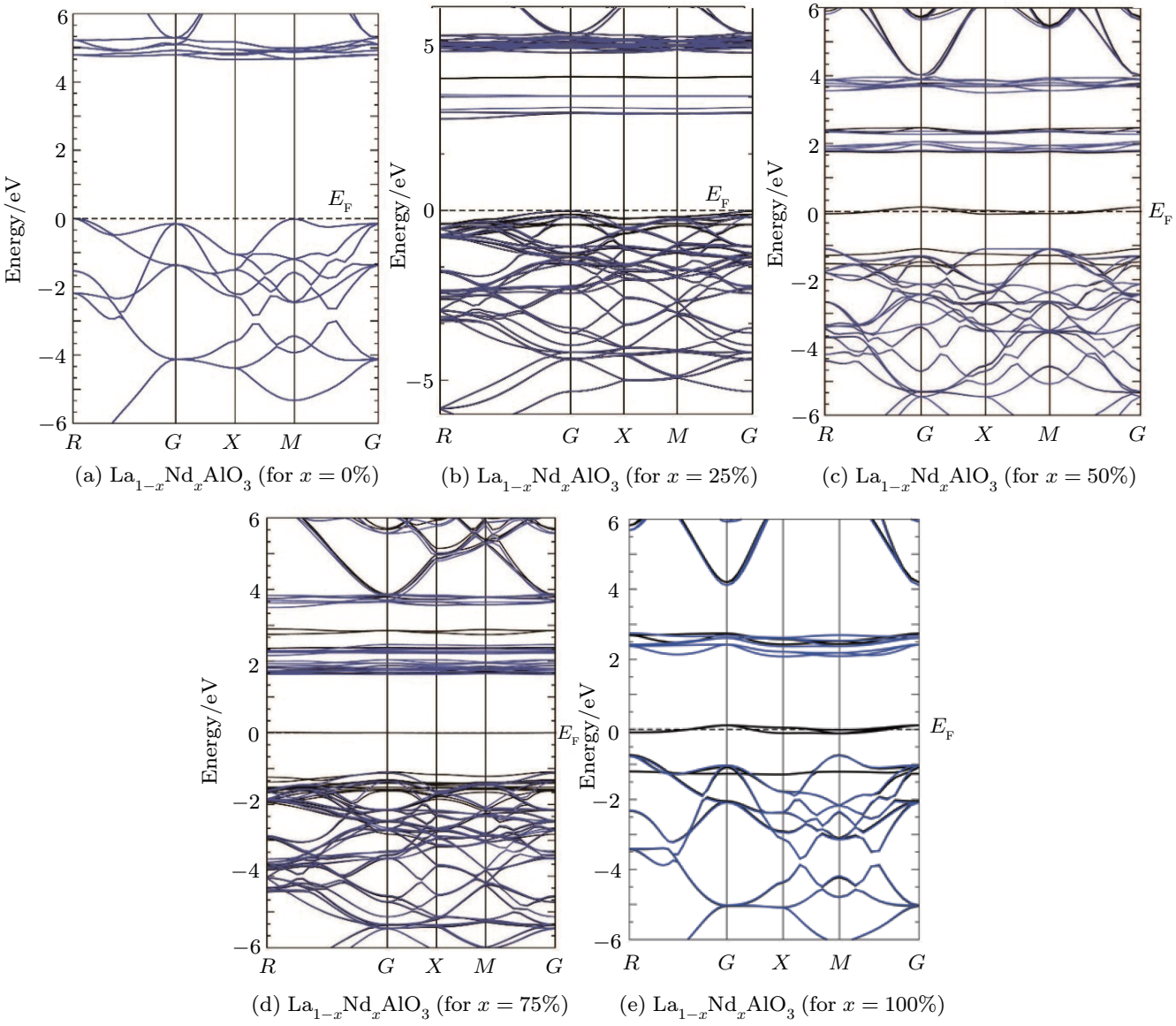

(a) $La_{1-x}Nd_xAlO_3$ (for $x = 0\%$) (b) $La_{1-x}Nd_xAlO_3$ (for $x = 25\%$) (c) $La_{1-x}Nd_xAlO_3$ (for $x = 50\%$)

(d) $La_{1-x}Nd_xAlO_3$ (for $x = 75\%$) (e) $La_{1-x}Nd_xAlO_3$ (for $x = 100\%$)

Fig. 5. Calculated band structures of the $La_{1-x}Nd_xAlO_3$ alloys at $x = 0\%$ (a), 25% (b), 50% (c), 75% (d), and 100% (e) in the spin-up (black) and the spin-down (blue) channels.

The band structures of the $La_{1-x}Nd_xAlO_3$ alloys at $x =$ 0%, 25%, 50%, 75%, and 100% displayed in Figs. 5(a)–5(e) show that for the concentrations at $x = 25\%$, 50%, and 75% the bands are more populated in the valence and conduction regions. The bands due to the La atoms are observed to be contributed in the conduction region and hence an insulating nature of $LaAlO_3$ is observed. With the doping of the Nd-atom in Figs. 5(a)–5(d), both the spin-up (black) and the spin-down (blue) bands are plotted. In these cases, the spin-up and spin-down band structures are metallic and insulating, respectively, suggesting their possible applications for spintronic devices.

4. Conclusions

In this paper, the spinpolarized modified Becke–Johnson potential used to calculate the electronic properties of the $La_{1-x}Nd_xAlO_3$ alloys with different Nd concentrations (at $x = 0\%$, 25%, 50%, 75%, and 100%). The observed electronic structures and the band features are explained each as a function of the concentration of the Nd-doped atom in $LaAlO_3$ where the Nd-4f state exchange splitting originates from the magnetic nature of the system. With the band structures of the spin-up and spin-down configurations exhibiting metallic and insulating characteristics respectively, this system may be suitably designed for half metallic magnetic devices. Furthermore, the significant variation of band gap with doping concentration may be useful in important spintronic and opto–electronic applications.

References

[1] Sales B C, Gschneidner K A Jr, Bunzli J C G, Pecharsky V K, Vasylechko L, Senyshyn A and Bismayer U 2003 *Handbook on the Physics and Chemistry of Rare Earths* (Amsterdam: Elsevier) Chap. 242

[2] Islam M S 2002 *Solid State Ionics* **154–155** 75

[3] Sangram K D and Binod K R 2015 *Chin. Phys. B* **24** 067702

[4] Liu Y K, Yin Y W and Li X G 2013 *Chin. Phys. B* **22** 087502

[5] Koren G, Gupta E, Giess A, Segmüller A and Laibowitz R B 1989 *Appl. Phys. Lett.* **54** 1054

[6] Zhang S B, Sun Y P, Zhao B C, Ang R, Zhu X B and Song W H 2009 *J. Alloys Compd.* **479** 22

[7] Henke M, Perßon J and Kück S 2000 *J. Lumin.* **87–89** 1049

[8] Bahoura M, Morris K J and Noginov M A 2002 *Opt. Commun.* **201** 405

[9] Maletic S, Maletic D, Petronijevic I, Dojcilovic J and Popovic D M 2014 *Chin. Phys. B* **23** 026102

[10] Cho S Y, Kim I T and Hong K S 1999 *J. Mater. Res.* **14** 114

[11] Huang C and Chen Y C 2002 *Mater. Res. Bull.* **37** 563

[12] Yang P, Shi M, Qin S and Deng H 2007 *Mater. Lett.* **61** 2687

[13] Liu X and Lin J 2009 *Solid State Sci.* **11** 2030

[14] Lybye D, Poulsen F W and Mogensen M 2009 *Solid State Ionics* **128** 91

[15] Yamasaka D, Tamagawa K and Ohki Y 2011 *J. Appl. Phys.* **110** 074103

[16] Ge J J, Yang M, Xue X B, You B, Sun L, Zhang W, Wu X S, Hu A and Du J 2012 *Phys. Status Solidi C* **9** 97

[17] Kuang X Y and Zhou K W 2000 *J. Phys. Chem. Solids* **61** 1225

[18] Wu G, Deng H, Wang W, Zhang K, Cao H, Yang P and Chu J 2014 *J. Mater. Sci.: Mater. Electron.* **25** 3137

[19] Liu H S, Fang X Y, Song W L, Hou Z L, Lu R, Yuan J and Cao M S 2009 *Chin. Phys. Lett.* **26** 067101

[20] Cheng F, Liu T Yu, Zhang Q R, Qiao H L and Zhou X W 2011 *Chin. Phys. Lett.* **28** 036106

[21] Lei S L, Li B, Huang J, Li Q X and Yang J L 2013 *Chin. Phys. Lett.* **30** 077502

[22] Hou Q Y, Li J J, Ying C, Zhao C W, Zhao E J and Zhang Y 2013 *Chin. Phys. B* **22** 077103

[23] Wang Q, Liang J F, Zhang R H, Li Q and Dai J F 2013 *Chin. Phys. B* **22** 057801

[24] Li S B, Yu H P, Zhang T1, Chen Z and Wu Z M 2014 *Chin. Phys. B* **23** 107101

[25] Zylberberg J and Zuo-Guang Y 2006 *J. Appl. Phys.* **100** 086102

[26] Murtaza G and Ahmad I 2012 *J. Appl. Phys.* **111** 123116

[27] Namjoo S, Rozatian A S H, Jabbari I and Puschnig P 2015 *Phys. Rev. B* **91** 205205

[28] Tran F and Blaha P 2009 *Phys. Rev. Lett.* **102** 226401

[29] Schwarz K and Blaha P 2003 *Comput. Mater. Sci.* **28** 259

[30] Sandeep, Ghimire M P and Thapa R K 2011 *J. Magn. Magn. Mater.* **323** 2883

[31] Blaha P, Schwarz K, Madsen G K H, Kvasnicka D and Luitz J 2001 *WIEN2k, An Augmented Plane Wave + Local Orbitals Program for Calculating Crystal Properties* Karlheinz Schwarz, Techn. Universitat Wien, Austria ISBN 3-9501031-1-2

[32] Wong K M, Alay-e-Abbas S M, Fang Y, Shaukat A and Lei Y 2013 *J. Appl. Phys.* **114** 034901

[33] Sandeep, Rai D P, Shankar A, Ghimire M P, Khenata R and Thapa R K 2015 *Phys. Scr.* **90** 065803

[34] Al-Sawai W, Lin H, Markiewicz R S, Wray L A, Xia Y, Xu S Y, Hasan M Z and Bansil 2010 *Phys. Rev. B* **82** 1

[35] Guo S D and Liu B G 2010 *Europhys. Lett.* **93** 47006

[36] Meinert M 2013 *Phys. Rev. B* **87** 1

[37] Yousaf M, Saeed M A, Ahmed R, Alsardia M M, Isa A R M and Shaari A 2012 *Commun. Theor. Phys.* **58** 777

[38] Araujo R B, De Almeida J S and Ferreira Da Silva A 2013 *J. Appl. Phys.* **114** 183702

[39] Perdew J P, Burke K and Ernzerhof M 1996 *Phys. Rev. Lett.* **77** 3865

[40] Sandeep, Rai D P, Shankar A, Ghimire M P, Khenata R and Thapa R K 2016 *Mod. Phys. Lett. B* **30** 1650028

[41] Wong K M, Alay-e-Abbas S M, Shaukat A, Fang Y and Lei Y 2013 *J. Appl. Phys.* **113** 014304

[42] Murnaghan F D 1944 *Proc. Natl. Acad. Sci. USA* **30** 244

[43] Boudali A, Saadaoui F, Zemouli M, DrissKhodja M D and Amara K 2013 *Adv. Mater. Phys. Chem.* **3** 146

[44] Bouvier P and Kreisel J 2002 *J. Phys.: Condens. Matter* **14** 3981

[45] Luo X and Wang B 2008 *J. Appl. Phys.* **104** 073518

[46] Ohtomo A and Hwang H Y 2004 *Nature* **427** 423

[47] Lim S G, Kriventsov S, Jackson T N, Haeni J H, Schlom D G, Balbashov A M, Uecker R, Reiche P, Freeouf J L and Lucovsky G 2002 *J. Appl. Phys.* **91** 4500

[48] Tang M J, Yang S Q, Liang T H, Yang Q X and Liu K 2013 *J. At. Mol. Sci.* **4** 280